Nuclear Instruments and Methods in Physics Research A 701 (2013) 214–220

Contents lists available at SciVerse ScienceDirect

Nuclear Instruments and Methods in Physics Research A

journal homepage: www.elsevier.com/locate/nima

Schottky barrier detectors on 4H-SiC n-type epitaxial layer for alpha particles

S.K. Chaudhuri, R.M. Krishna, K.J. Zavalla, K.C. Mandal *

Department of Electrical Engineering, University of South Carolina, Columbia, SC 29208, USA

ARTICLE INFO

Article history:
Received 14 September 2012
Received in revised form
25 October 2012
Accepted 5 November 2012
Available online 16 November 2012

Keywords:
4H-SiC
Schottky barrier
Alpha particle detection
Diffusion model
Biparametric correlation

ABSTRACT

Schottky barrier detectors have been fabricated on 50 μm n-type 4H-SiC epitaxial layers grown on 360 μm SiC substrates by depositing ~10 nm nickel contact. Current–voltage (*I–V*) and capacitance–voltage (*C–V*) measurements were carried out to investigate the Schottky barrier properties. The detectors were evaluated for alpha particle detection using a ^{241}Am alpha source. An energy resolution of ~2.7% was obtained with a reverse bias of 100 V for 5.48 MeV alpha particles. The measured charge collection efficiency (*CCE*) was seen to vary as a function of bias voltage following a minority carrier diffusion model. Using this model, a diffusion length of ~3.5 μm for holes was numerically calculated from the *CCE* vs. bias voltage plot. Rise-time measurements of digitally recorded charge pulses for the 5.48 MeV alpha particles showed a presence of two sets of events having different rise-times at a higher bias of 200 V. A biparametric correlation scheme was successfully implemented for the first time to visualize the correlated pulse-height distribution of the events with different rise-times. Using the rise-time measurements and the biparametric plots, the observed variation of energy resolution with applied bias was explained.

1. Introduction

Designing and fabrication of high resolution nuclear radiation detectors based on silicon carbide (SiC) epilayers have recently attracted a great deal of attention in the field of nuclear isotope identification and detection [1–5]. SiC epilayers offer high crystallinity, higher growth controllability and reproducibility compared to its bulk counterpart. Properties like wide band-gap, radiation hardness and high breakdown field make SiC a potential candidate for radiation detectors even in harsh environments such as high radiation background and hot and humid environments, without considerable deterioration in their detection properties. Because of its wide band-gap (3.27 eV at 300 K), 4H-SiC devices exhibit extremely low leakage currents and hence can be used for high-resolution radiation detection measurements at room temperature as well as at elevated temperatures [6–8]. Polytype 4H-SiC has a very high threshold displacement energy (22–35 eV) which accounts for its high radiation hardness [9,10].

The presence of defects in the epilayer and the substrate is one of the crucial factors which define the performance of the SiC detectors. Major defects present in SiC are edge dislocations, screw dislocations, carrot defects, comet defects, triangular defects, and basal plane dislocations [11–13]. Most of these defects are normally confined to the substrate [14] but some screw dislocations can propagate to the epitaxial layer and form micropipe defects in the epilayer [15]. A sufficiently large depletion width, which defines the active volume of the detector, is yet another crucial requirement for obtaining high energy resolution and high efficiency detection.

The prospect of SiC Schottky diodes as alpha particle detectors was first reported by Babcock and Chang [6]. Ruddy et al. [16], reported a resolution of 5.8% (full width at half maxima, FWHM) at a deposited energy of 294 keV and 6.6% (FWHM) at a deposited energy of 260 keV by alpha particles from a collimated ^{238}Pu source in 4H-SiC Schottky diodes with circular contacts of diameter 200 and 400 μm. Nava et al. [8] reported very robust 5.48 MeV alpha particle signal in 4H-SiC epitaxial detectors with circular contacts of ~2 mm diameter. However, they have not achieved a saturation of the charge collection efficiency even at a bias voltage of 200 V. In a later work [17], Ruddy et al. reported an energy resolution of 5.7% for a deposited energy of 89.5 keV alpha particles from a 100 μm collimated ^{148}Gd source in similar detectors with relatively larger Schottky contact diameter of 2.5, 3.5, 4.5 and 6.0 mm and 10 μm thick epilayer. Among high resolution alpha particle detection reports, Ruddy et al. [1] reported fabrication of alpha particle detectors with aluminum guard ring structures using which they obtained an energy resolution close to 46 keV for alpha particles from a ^{238}Pu source and 41.5 keV for alpha particles from a ^{148}Ga source. Ivanov et al. [5] reported an energy resolution of 20 keV in the energy range 5.4–5.5 MeV. In another work, Ruddy et al. [18] reported an energy resolution of 20.6 keV for ^{238}Pu alpha

* Corresponding author. Tel.: +1 803 777 2722; fax: +1 803 777 8045.
E-mail address: mandalk@cec.sc.edu (K.C. Mandal).

0168-9002/$ - see front matter © 2012 Elsevier B.V. All rights reserved.
http://dx.doi.org/10.1016/j.nima.2012.11.015

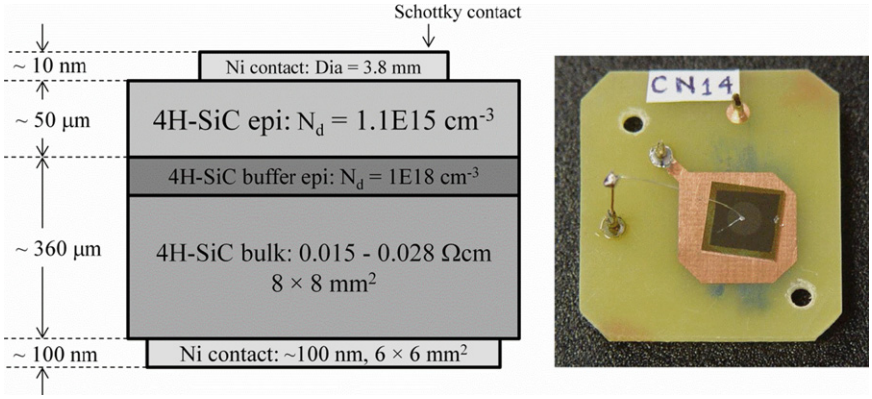

Fig. 1. Schematic diagram of n-type 4H-SiC epilayer Schottky barrier detector and a photograph of an actual detector mounted on a PCB and wire bonded.

particles and Pullia et al. [19] reported 0.9% energy resolution in the 4.8–5.8 MeV energy range at a temperature of 55 °C using a SiC/GaN detector with a 1000 Å Au entrance window.

In this article, we describe the fabrication of low-leakage radiation detector on 4H-SiC n-type epilayer and a systematic study of its performance as an alpha particle detector. The detector has been characterized using *I–V*, *C–V*, and alpha ray spectroscopic measurements. The room temperature *I–V* measurements revealed a very low leakage current of ~0.8 nA at 250 V reverse bias. Charge collection efficiencies (*CCE*) were measured as a function of bias voltage for 5.48 MeV alpha particles. Using the experimentally obtained *CCE* values and a minority carrier diffusion model, contribution of hole diffusion to the charge collection efficiency values and the hole diffusion length has been numerically calculated. Digital spectroscopic methods were adopted to obtain the rise-time of pulses and biparametric correlation plots. Using the rise-time distribution and the biparametric plots, the observed increase in FWHM values for the alpha particles at higher bias has been explained.

2. Experimental

2.1. Detector fabrication

We have used 50 μm thick n-type epitaxial layer grown on a 50 mm diameter 4H-SiC (0 0 0 1) wafer, highly doped with nitrogen and 8° off-cut towards the [1 1 $\bar{2}$ 0] direction. The net doping concentration of the epitaxial layer measured using the high frequency (100 kHz) capacitance–voltage (*C–V*) method was found to be 1.1×10^{15} cm^{-3}. A micropipe defect density less than 15 cm^{-2} has been evaluated using Nomarski optical microscopy and scanning electron microscopy (Quanta 200 SEM, low vacuum mode) on a sister sample. The radiation detectors were fabricated on 8×8 mm^2 substrates diced from the 50 mm diameter wafer by depositing 3.8 mm diameter Ni Schottky contacts ~10 nm in thickness on top of the epitaxial layers through the shadow mask using a Quorum model Q150T sputtering unit. Large Ni contact (approx. 6×6 mm^2) 100 nm in thickness was deposited on the opposite surface for the back contact. Standard RCA cleaning procedure of the wafer was carried out prior to the contact deposition. The wafer was then mounted on a printed circuit board (PCB) and wire bonded for proper electrical connection. Fig. 1 shows a schematic diagram of the detector and a photograph of the detector fabricated for the present studies.

2.2. Electrical characterization

Current–voltage (*I–V*) measurements were carried out on these detectors using a Keithley 237 sourcemeter. Forward and reverse bias characteristics were acquired to obtain the diode parameters and leakage current. Capacitance–voltage (*C–V*) measurements were carried out using a Keithley 590 CV analyzer at a frequency of 100 kHz. The effective doping concentration was calculated using standard $1/C^2$ vs. *V* plots. All measurements were carried out at room temperature.

2.3. Alpha spectroscopy

Pulse-height spectra of alpha particles from a 0.1 μCi ^{241}Am alpha source were recorded using a standard analog spectrometer. The source and the detector were placed inside an EMI shielded aluminum box which was constantly evacuated using a rotary pump in order to minimize scattering of alpha particle with air molecules. The source used was a broad window (2 mm) source kept at a distance of 1.5 cm from the detector window ensuring that the whole surface of the detector was illuminated. The detector signals were collected using a Cremat CR110 charge sensitive pre-amplifier. The charge pulses were shaped using an Ortec 572 spectroscopy amplifier. The amplified signals were then digitized and binned to obtain pulse-height spectra using a Canberra Multiport II ADC-MCA unit controlled by Genie 2000 interface software. The peaks obtained in various spectra were fitted using peak analyzer function of Origin 8.6. Charge collection efficiencies (*CCE*) were measured using the same alpha source at different reverse bias voltages as the ratio of energy deposited in the detector to the actual energy of particles (5.48 MeV) emitted by the source. The energy deposited was calculated from the alpha peak position in a calibrated MCA.

Digital spectroscopic measurements were accomplished using a GWInstek (GDS1062A) digital oscilloscope used as a digitizer with a sampling rate of 1 MS/s and 8 bit ADC resolution. The pre-amplifier pulses were digitized and recorded in a PC for offline analysis. At least 5000 pulses were recorded to obtain decent statistics. The data acquisition and the offline analysis software were designed in-house using the LabVIEW and MATLAB programming languages, respectively. The analyses involved calculation of the 10%–90% rise-time of the charge pulses and pulse-height determination after shaping the pre-amplifier signal. The Gaussian shaping of the pulses were achieved using a transfer function resembling CR-RC^4 semi-Gaussian configuration. The software was also used to obtain distributions of pulse-height and rise-time and biparametric plots to investigate any type of

correlation between the pulse-heights and pulse-shapes of a set of events.

3. Results and discussions

3.1. Electrical measurements

Fig. 2 shows I–V characteristics of the detector at forward and reverse bias. The room temperature reverse bias leakage current was found to be ~0.8 nA at a bias voltage of 250 V and ~0.2 nA at 100 V. A diode ideality factor of 1.4 and a Schottky barrier height of 1.3 eV was found from the forward I–V characteristic and using a thermionic emission model [20] given by

$$I = I_S\left(e^{\beta V_a/n} - 1\right) \tag{1}$$

where I_S is the saturation current, V_a is the applied voltage, n is the diode ideality factor and $\beta = q/k_BT$, q being the electronic charge, k_B the Boltzmann constant, and T is the absolute temperature. The saturation current is given by

$$I_s = A^*AT^2\left(e^{-\beta\varphi_B}\right) \tag{2}$$

where A^* is the effective Richardson constant (146 A cm^{-2} K^{-2} for 4H-SiC), A is the area of the diode, φ_B is the Schottky barrier height and n is the diode ideality factor.

The barrier height thus calculated depends on the spatial homogeneity of the Schottky barrier height [21]. An ideality factor greater than unity, indicates non-uniformity in the surface barrier height, which in turn indicates the possibility of the presence of traps in the depletion region [22].

Fig. 3 shows a $1/C^2$ vs. V_a plot obtained for the present detector. A linear fit to the curve gives an effective doping concentration value $N_{eff} = 1.1 \times 10^{15}$ cm^{-3} and a built-in potential (V_{bi}) of 1.4 V. The barrier height was also calculated from the C–V characteristics to be 1.47 eV, using the equations given below

$$\phi_{B(C-V)} = V_{bi} + V_n \tag{3}$$

where, V_n is the potential difference between the Fermi level energy and the bottom of the conduction band in the neutral region of the semiconductor and is given by

$$V_n = kT\ln\frac{N_C}{N_D} \tag{4}$$

where N_C is the effective density of states in the conduction band of 4H-SiC and is taken equal to 1.6×10^{19} cm^{-3} [23]. The barrier height calculated from the C–V measurements is slightly higher than that obtained from the forward I–V characteristics. The value of barrier height obtained from forward I–V characteristics is dominated by low Schottky barrier height locations in an inhomogeneous Schottky diode. So, the barrier height thus calculated shows lower values than that obtained from C–V characteristics, which on the other hand gives an average value of the barrier height for the whole diode [24]. Hence, the larger value of barrier height calculated from the C–V measurements further confirms the inhomogeneity of the surface barrier height.

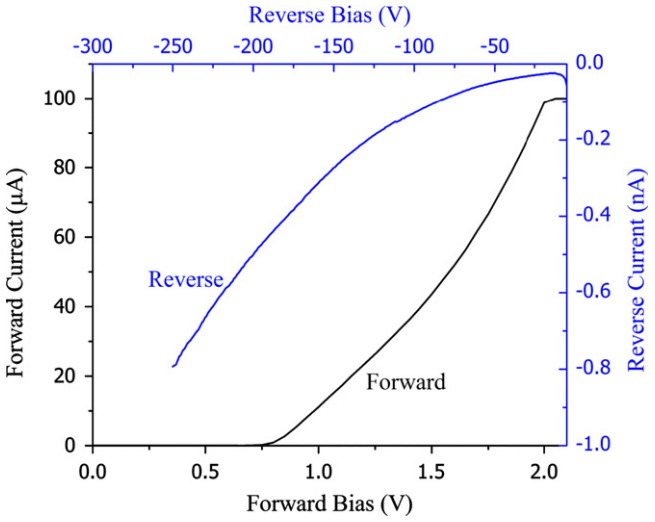

Fig. 2. Room temperature I–V characteristics at forward and reverse bias for n-type 4H-SiC epitaxial Schottky detector.

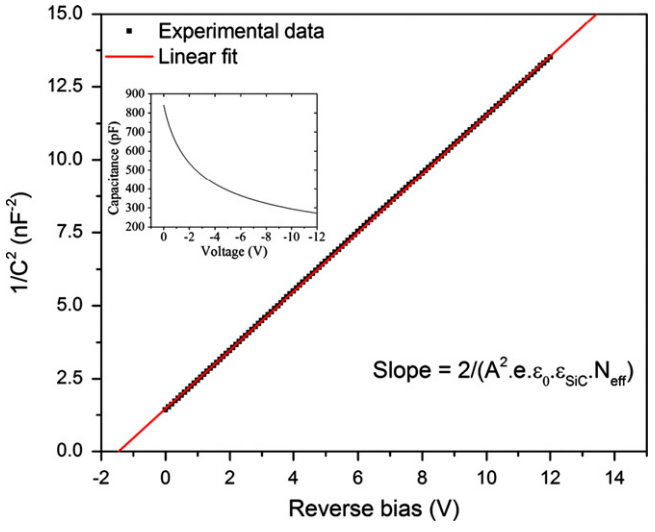

Fig. 3. $1/C^2$ vs. V plot for n-type epitaxial 4H-SiC Schottky barrier detector. The solid line shows the linear fit to the experimental data. Effective doping concentration (N_{eff}) is derived from the slope of the linear fit and using the formula shown, where A is the area, e is the electronic charge, ε_0 is permittivity of vacuum and ε_{SiC} is the dielectric constant of 4H-SiC. The original C–V plot has been shown in the inset.

3.2. Alpha spectroscopic measurements

Fig. 4 shows a pulse-height spectrum obtained using a ^{241}Am alpha source at zero applied bias (V_a+1.4 V=0 V). A symmetric

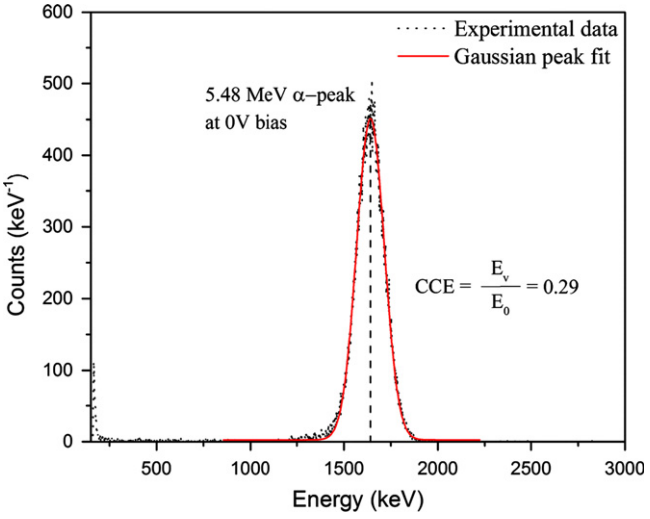

Fig. 4. Pulse-height spectrum obtained for 5.48 MeV alpha particles from a ^{241}Am source using n-type 4H-SiC epitaxial Schottky barrier detector biased at 0 V. The dotted line shows the peak centroid, E_v and E_0 is the actual energy (5.48 MeV) of the emitted alpha particles.

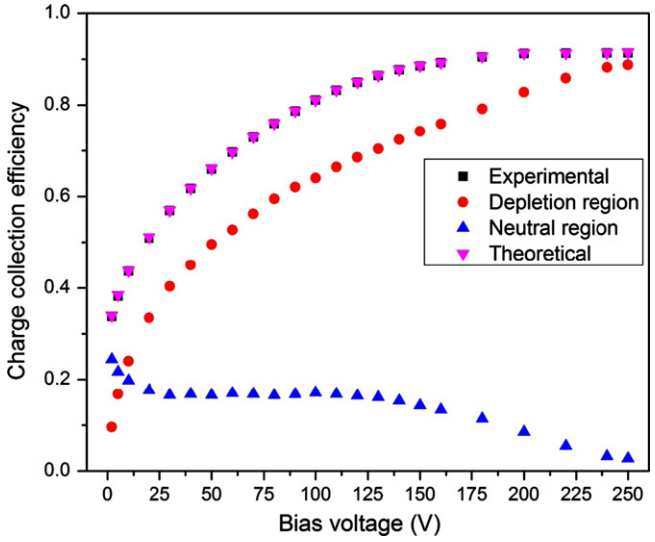

Fig. 5. Variation of experimentally obtained (■) and theoretically calculated (▼) charge collection efficiency as a function of reverse bias voltage. The theoretically calculated separate contributions to the total *CCE* from charge drifts in depletion region (●) and from hole diffusion in neutral region (▲) are also shown.

and robust peak was obtained which indicates a substantial amount of diffusion of minority carriers. At zero applied bias, because of the negligible width of the depletion region, all the interactions predominantly take place in the neutral region (beyond the depletion region) as the range of 5.48 MeV alpha particles in SiC is ~18 μm. So, the charge transfer is dominated by the diffusion of holes. The charge collection efficiency at zero applied bias in this case was calculated to be 29%. Such a high value of *CCE* at zero applied bias implies that the diffusion length of the holes is comparable to the range of the alpha particles. Ivanov et al. [25] have reported an even higher *CCE* of 50% at 0 V in their 26 μm thick n-type 4H-SiC epilayer detectors for 5.39 MeV alpha particles. The hole diffusion length in their case was reported as 13.2 μm. Fig. 5 shows the variation of *CCE* calculated using 5.48 MeV alpha particles as a function of reverse bias voltage. The *CCE* was seen to saturate after an applied reverse voltage of 180 V. The highest *CCE* achieved was 92% at 250 V. The reason behind not achieving 100% *CCE* can be explained as follows. The depletion width at a reverse bias of 250 V was calculated to be 16 μm. Alpha particles of energy 5.48 MeV have a projected range of 18 μm in SiC. So the alpha particles do not deposit their full energy in the depletion region which is the active region of the detector and hence 100% efficiency was not observed. To have a better perspective of the variation of *CCE* with applied bias, we calculated the separate contribution of charge carriers produced in the depletion region and that of the diffusion of holes created in the neutral region, to the observed *CCE*. The calculation was done based on a model proposed by Breese [26] originally for calculating minority carrier diffusion length for ion beam induced charge collection measurements. According to the model, the charge collection efficiency at a given reverse bias voltage (depletion width) is given as

$$CCE_{theory} = \frac{1}{E_p}\int_0^d \left(\frac{dE}{dx}\right)dx + \frac{1}{E_p}\int_d^{x_r}\left[\left(\frac{dE}{dx}\right)\times \exp\left\{-\frac{(x-d)}{L_d}\right\}\right]dx$$
$$= CCE_{depletion} + CCE_{diffusion} \quad (5)$$

where E_p is the energy of the alpha particles, d is the depletion width at the particular bias, dE/dx is the electronic stopping power of the alpha particles calculated using SRIM 2012 [27], x_r is the projected range of the alpha particles with energy E_p and L_d is the diffusion length of the minority carriers. The first term of Eq. (5), $CCE_{depletion}$, gives the contribution of charge generated within the depletion region to the charge collection efficiency and the second term, $CCE_{diffusion}$, is that from the charge carriers created in the region behind the depletion region and diffused to the depletion region. The diffusion length of the holes was calculated as follows. First $CCE_{depletion}$ was calculated by numerically integrating the dE/dx values obtained from SRIM 2012 (See Eq. (5)) at a particular bias voltage. Then $CCE_{diffusion}$ and L_d, was calculated while considering L_d as a free parameter to fit the experimentally obtained *CCE* value at that particular bias. The average L_d value obtained considering all the bias voltages was calculated to be 3.5 μm. Similar calculation was reported by Manfredotti et al. [28] where they numerically fit the experimentally obtained *CCE* values by calculating the *CCE* theoretically while considering L_d as a free parameter. Fig. 5 also plots separately the values of $CCE_{depletion}$, $CCE_{diffusion}$, and CCE_{theory}. It can be seen from the figure that initially (up to 5 V), the $CCE_{diffusion}$ values were higher than $CCE_{depletion}$ values, which implies that at lower biases the charge transport was dominated by hole diffusion. Similarly, it can be seen that at higher biases the $CCE_{depletion}$ values almost matches the experimentally obtained *CCE* values which implies that the charge transfer is almost solely due to carrier drift inside the depletion region.

Apart from the *CCE*, the energy resolution was also monitored as a function of bias voltage. Fig. 6 shows the variation of detector resolution measured in terms of FWHM as well as percentage resolution, for 5.48 MeV peak, as a function of reverse bias voltage. Also, Table 1 lists the peak parameters for some of the important cases relevant to the discussion. In order to monitor any variation in the post-detector electronics, pulser spectra were simultaneously recorded during all the data acquisitions using

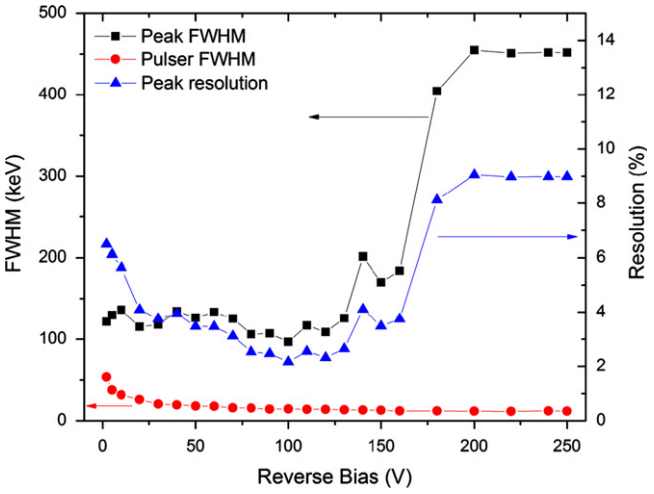

Fig. 6. Variation of 5.48 MeV alpha peak FWHM (■), pulser peak FWHM (●) and alpha peak percentage resolution (▲) as a function of detector bias voltage. The solid lines are guide to eyes.

Table 1
Alpha peak parameters at different bias voltages.

Applied bias (V)	Average energy (keV)	Energy resolution	
		keV	%
0	1262.0	133.4	10.6
100	4528.7	122.2	2.7
200	5006.6	454.8	9.1

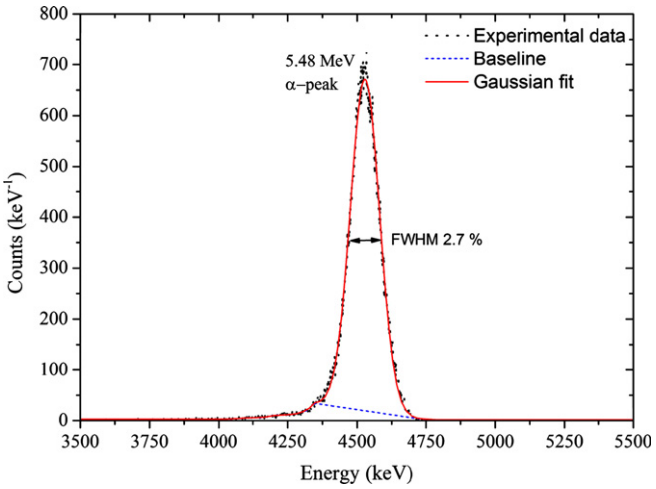

Fig. 7. Pulse-height spectra obtained using the n-type 4H-SiC Schottky barrier detector for 5.48 MeV alpha particles at an operating voltage of 100 V. The dots are the experimental points and the solid line is a Gaussian distribution fitted to the experimental data. The dashed line shows the baseline.

a precision pulser. The pulser peak FWHM essentially gives the magnitude of noise of the detection system. Fig. 6 also shows the variation of the pulser FWHM as a function of bias voltage. The much higher FWHM values of alpha peak compared to that of the pulser peak clearly indicates that the detector resolution was not limited by the overall electronic noise of the system. It can be seen from the figure that initially the resolution improved with increase in bias voltage, attained a minima at 100 V and then started increasing with increasing bias. Fig. 7 shows the alpha pulse-height spectrum obtained at 100 V. The percentage resolution was calculated to be 2.7%. The initial decrease in the FWHM value is a normal detector behavior and is generally attributed to the increase in the active volume of the detector and reduction in detector capacitance with increase in bias. The reason behind the increase in the FWHM values beyond 100 V was not very apparent. No variation in the pulser peak FWHM was observed in this region. Thus the effect of increasing leakage current on the detector resolution with applied bias can be ruled out as increase in detector leakage current means increase in parallel noise which would broaden the pulser peak as well. A plausible reason behind the deterioration of resolution with increasing bias could be explained as follows. As the reverse bias increases, the depletion region extends more towards the epilayer-substrate interface. So, the probability of finding threading type dislocation defects increases more and more. Threading dislocations are basically dislocations which propagate from the substrate to the epilayer.

In order to have a deeper understanding, pulse-height and rise-times measurements of the alpha particle charge pulses from the detector were carried out. The variations of rise-times were observed for the detector biased at two different voltages. Fig. 8(a) and (b) shows the 10%–90% rise-time distribution histogram at 100 and 200 V respectively. A Gaussian fit to the distribution showed that the rise-time distribution for the alpha particle charge pulses was centered at around 69 ns when the detector was biased at 100 V. Interestingly, Fig. 8(b) shows a clear presence of two peaks in the rise-time distribution of pulses acquired at 200 V. The histogram was fitted with a two-Gaussian peak fit function and the two peaks were found to be centered at 64 and 52 ns. So, it appears that an additional set of events with faster rise-time is present. If we consider our previous assumption of inclusion of defect-rich region with higher bias to be true, then it can be assumed that a fraction of the charge carriers are getting trapped and recombining in these defects. As a result of this, these

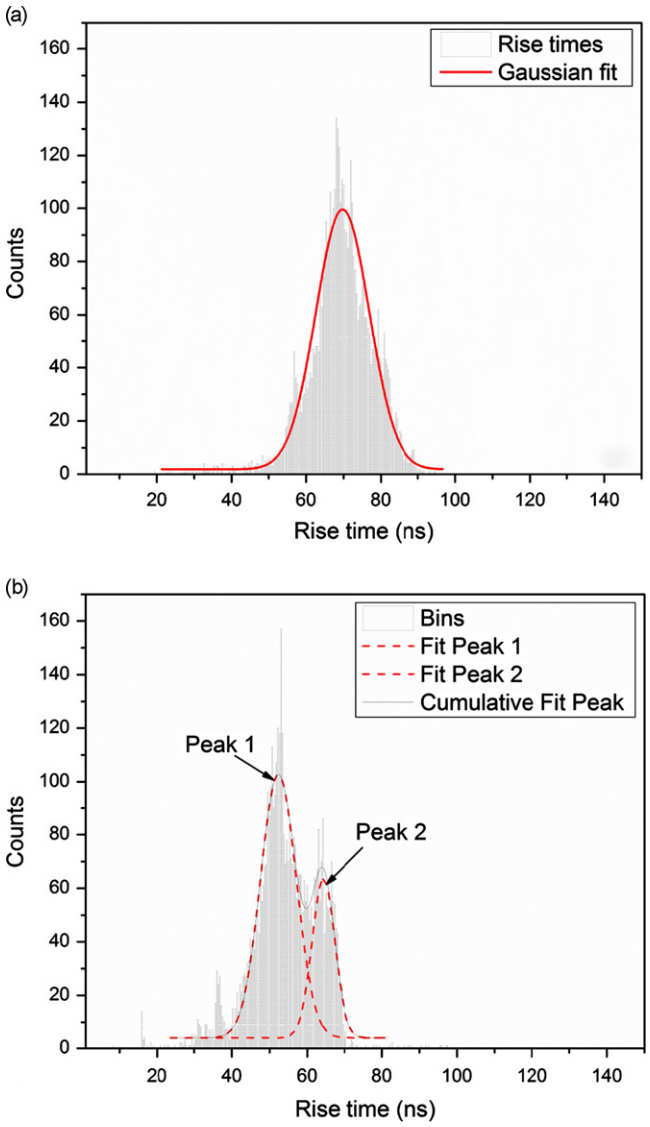

Fig. 8. Distribution of 10%–90% rise-time of charge pulses obtained for 5.48 MeV alpha particles when the detector was biased at 100 V (a) and at 200 V (b). In order to obtain the peak positions, the peaks were fitted with Gaussian functions.

charges never reach the collecting electrode and hence induce partial charge on the collecting electrode. As a consequence, the 10%–90% rise-time calculated from these pulses turn out to be faster. This can be very easily visualized using biparametric plots. A biparametric plot is a two dimensional graph showing the correlation between two pulse parameters of a set of pulses [28,29]. Fig. 9(a) and (b) shows the biparametric plot obtained for two different detector biasing, 100 and 200 V respectively. The pulse-height and the pulse rise-time for each event are plotted on the horizontal and vertical axes respectively and the number of events is displayed by the graded color (black being low and white being high). In Fig. 9(a), a spot of events were observed which corresponds to the 5.48 MeV alpha particles. On the other hand in Fig. 9(b), a very broad set of correlated events could be noticed. We have tried to spot the correlation events corresponding to the two rise-times as shown by the dotted ellipses. The broadness in the corresponding pulse-height distribution is possibly due to the variation of the induced charge due to uneven radial distribution of defect concentration. It can also be seen from Fig. 9(b) that the pulse-height distribution corresponding to the set of events with lower rise-times values (lower band) is

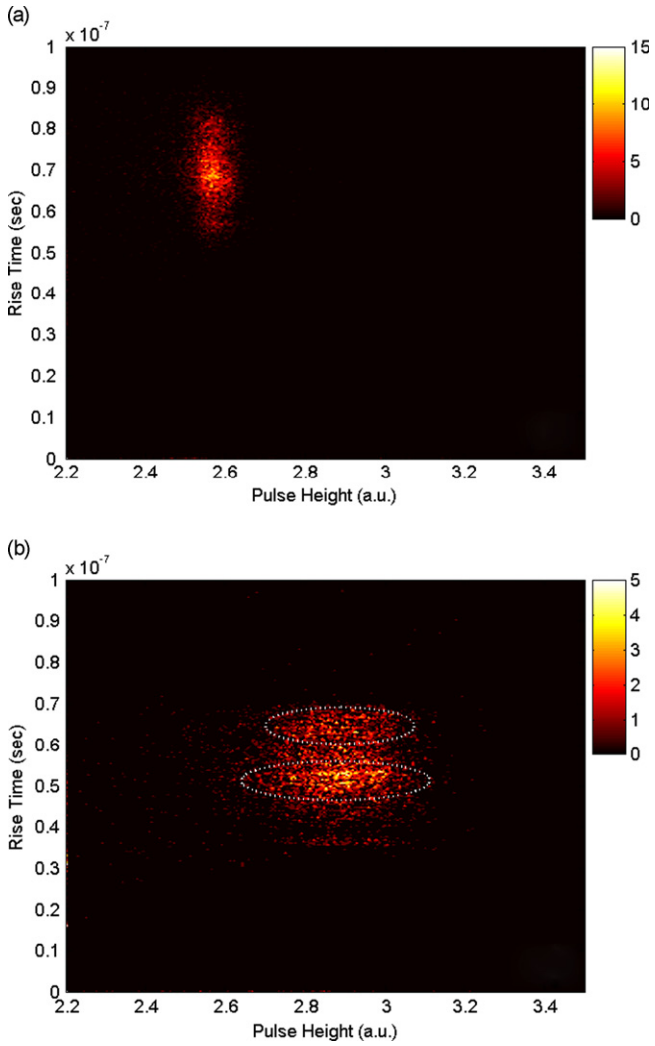

Fig. 9. Biparametric plots showing the correlation of pulse-height and rise-time of charge pulses obtained for 5.48 MeV alpha particles when the detector was biased at 100 V (a) and at 200 V (b).

broader than that of the set of events with higher rise-time (upper band) which also confirms our assumption of variation in charge induced by the carriers trapped in defects. The widening of the alpha peak at higher bias can be realized easily from the biparametric plot. The pulse-height spectrum can be visualized as a projection of the number of these counts on the pulse-height axis of the biparametric plot. In the case of the higher bias, because of the overall broadening of the distribution of energy, the resulting projection on the *x*-axis returns a broad energy peak.

Finally, it should be mentioned that various factors regulate the energy resolution of this kind of 4H-SiC epitaxial Schottky barrier radiation detectors. Presence of defects like micropipes in the epilayer is the most serious concern as of now. The superior energy resolution obtained in the present work is believed mostly due to the low concentration of micropipes. Also various authors have reported [1,5,18,19] that the ultimate energy resolution of the detector is limited by the energy dispersion at the metal contact window. Therefore, the choice of window material and optimization of the window thickness also plays a very important role for obtaining high energy resolution. The measured energy resolution also depends on the variation of angle of incidence of the gamma rays. Since a broad source has been used in this study a further improvement in the detector performance can be expected if a collimated source is being used.

4. Conclusions

The performances of radiation detectors fabricated from 4H-SiC n-type epilayers on SiC substrates were evaluated for alpha particle detection. An energy resolution of 2.7% of ^{241}Am (5.48 MeV) alpha particles was obtained for full illumination of the detector at an optimized bias of 100 V using a simple planar structure. *I–V* measurements at room temperature have showed very low ($\sim$0.8 nA at 250 V) leakage current. Although the charge collection efficiency of the detector was seen to increase with bias voltages beyond 100 V, the FWHM value for the 5.48 MeV alpha particles was seen to degrade with further increment in bias voltages. A theoretical investigation of *CCE* variation with applied bias was carried out to study the contribution of hole diffusion to the charge collection process. From this study, the diffusion length of holes was calculated to be 3.5 μm. Distribution of rise-time of the pulses obtained by the detector biased at 200 V, showed a presence of two sets of pulses with different rise-times. From a biparametric correlation plot, these two sets of events were found to have different pulse-height distribution. Inclusion of more and more defects into the detector active volume due to the increase in depletion width with increase in reverse bias was considered to be a possible reason for the observed higher FWHM values at higher reverse bias voltages.

Acknowledgments

One of the authors (KCM) acknowledges partial financial support provided by Los Alamos National Laboratory/DOE (Grant no. 143479). Authors are thankful to Professor T.S. Sudarshan of Electrical Engineering department for providing the electrical characterization laboratory facilities. The authors are also thankful to Dr. Peter G. Muzykov for his help and suggestions.

References

[1] F.H. Ruddy, J.G. Seidel, H. Chen, A.R. Dulloo, Sei-Hyung Ryu, IEEE Transactions on Nuclear Science NS 53 (2006) 1713.
[2] K.C. Mandal, P.G. Muzykov, J.R. Terry, Applied Physics Letters 101 (2012) 051111.
[3] K.C. Mandal, P.G. Muzykov, R.M. Krishna, J.R. Terry, IEEE Transactions on Nuclear Science NS 59 (2012) 1591.
[4] G. Bertuccio, R. Casiraghi, A. Cetronio, C. Lanzieri, F. Nava, Nuclear Instruments and Methods in Physics Research Section A 522 (2004) 413.
[5] A. Ivanov, E. Kalinina, G. Kholuyanov, N. Strokan, G. Onushkin, A. Konstantinov, A. Hallen, A. Kuznetsov, in: R. Nipoti, A. Poggi, A. Scorzoni (Eds.), Proceedings of the 5th European Conference on Silicon Carbide and Related Materials 2004, Trans Tech Publications Inc., Zurich, Switzerland, 2005, p. 1029.
[6] R.V. Babcock, H.C. Chang, Proceedings of the Symposium on Neutron Detection, Dosimetry and Standardization, December 1962, vol. 1, International Atomic Energy Agency (IAEA), Vienna, 1962 p. 613.
[7] A.R. Dulloo, F.H. Ruddy, J.G. Seidel, C. Davison, T. Flinchbaugh, T. Daubenspeck, IEEE Transactions on Nuclear Science NS 46 (1999) 275.
[8] F. Nava, P. Vanni, C. Lanzieri, C. Canali, Nuclear Instruments and Methods in Physics Research Section A 437 (1999) 354.
[9] G. Lucas, L. Pizzagalli, Nuclear Instruments and Methods in Physics Research Section B 229 (2005) 359.
[10] F. Nava, G. Bertuccio, A. Cavallini, E. Vittone, Measurement Science and Technology 19 (2008) 102001.
[11] F. Moscatelli, A. Scorzoni, A. Poggi, M. Bruzzi, S. Sciortino, S. Lagomarsino, G. Wagner, I. Mandic, R. Nipoti, IEEE Transactions on Nuclear Science NS 53 (2006) 1557.
[12] K.C. Mandal, R.M. Krishna, P.G. Muzykov, S. Das, T.S. Sudarshan, IEEE Transactions on Nuclear Science NS 58 (2011) 1992.
[13] P.G. Muzykov, R.M. Krishna, K.C. Mandal, Journal of Applied Physics 111 (2012) 014910.
[14] S. Wang, M. Dudley, C.H. Carter Jr., H.S. Kong, Materials Research Society Symposium Proceedings 339 (1994) 735.
[15] Q. Wahab, A. Ellison, C. Hallin, A. Henry, J. Di Persio, R. Martinez, E. Janzén, Materials Science Forum 338 (2000) 1175.
[16] F.H. Ruddy, A.R. Dulloo, J.G. Seidel, S. Seshadri, L.B. Rowland, IEEE Transactions on Nuclear Science NS 45 (1998) 536.

[17] F.H. Ruddy, A.R. Dulloo, J.G. Seidel, J.W. Palmour, R. Singh, Nuclear Instruments and Methods in Physics Research Section A 505 (2003) 159.
[18] F.H. Ruddy, J.G. Seidel, P. Sellin, Proceedings of the IEEE Nuclear Science Symposium Conference Record (NSS/MIC), 2009, p. 2201.
[19] A. Pullia, G. Bertuccio, D. Maiocchi, S. Caccia, F. Zocca, IEEE Transactions on Nuclear Science NS 55 (2008) 3736.
[20] E.H. Rhoderick, R.H. Williams, Metal-Semiconductor Contacts, Clarendon, Oxford, 1988.
[21] R.T. Tung, Physical Review B 45 (1992) 13509.
[22] P.G. Muzykov, R.M. Krishna, K.C. Mandal, Applied Physics Letters 100 (2012) 032101.
[23] M. Jang, Y. Kim, J. Shin, S. Lee, IEEE Electron Device Letters 26 (2005) 354.
[24] 〈http://www.ioffe.rssi.ru/SVA/NSM/Semicond/SiC/bandstr.html〉.
[25] A.M. Ivanov, E.V. Kalinina, A.O. Konstantinova, G.A. Onushkin, N.B. Strokan, G.F. Kholuyanov, A. Hallén, Technical Physics Letters 30 (2004) 1.
[26] M.B.H. Breese, Journal of Applied Physics 74 (1993) 3789.
[27] J.F. Ziegler, J. Biersack, U. Littmark, The Stopping and Range of Ions in Matter, Pergamon Press, New York, 1985.
[28] C. Manfredotti, F. Fizzotti, A. Lo Giudice, C. Paolini, E. Vittone, F. Nava, Applied Surface Science 184 (2001) 448.
[29] S.K. Chaudhuri, A. Lohstroh, M. Nakhostin, P.J. Sellin, Journal of Instrumentation 7 (2012) T04002.